Parametric Amplification and Self-Oscillation in a Nanotube Mechanical Resonator

Alexander Eichler, Julien Chaste, Joel Moser, and Adrian Bachtold*

Catalan Institute of Nanotechnology (ICN) and CIN2, Campus UAB, 08193 Bellaterra, Barcelona, Spain

S Supporting Information

ABSTRACT: A hallmark of mechanical resonators made from a single nanotube is that the resonance frequency can be widely tuned. Here, we take advantage of this property to realize parametric amplification and self-oscillation. The gain of the parametric amplification can be as high as 18.2 dB and tends to saturate at high parametric pumping due to nonlinear damping. These measurements allow us to determine the coefficient of the linear damping force. The corresponding damping rate is lower than the one obtained from the line shape of the resonance (without pumping), supporting the recently reported scenario that describes damping in nanotube resonators by a nonlinear force. The possibility to combine nanotube resonant mechanics and parametric amplification holds promise for future ultralow force sensing experiments.

KEYWORDS: Nanoelectromechanical systems, mechanical resonators, carbon nanotubes, parametric amplification, nonlinear damping
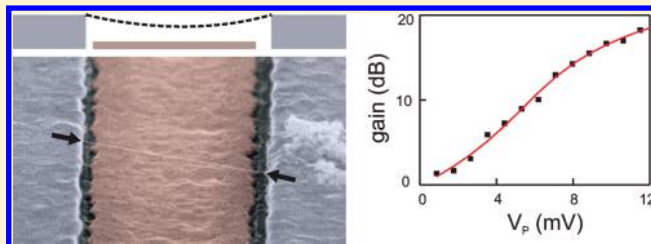
Carbon nanotubes allow the fabrication of nanoelectromechanical resonators with outstanding properties. The resonance frequency can be very high[1] and at the same time widely tunable.[2,3] In addition, nanotube resonators are very sensitive to electron charges,[4,5] to mass,[6−8] and to force.[9] A major issue in these experiments is the detection of the motion. The difficulty lies in transducing the high-frequency subnanometer amplitude of the motion into a sizable electrical signal. This is especially true for ultrasensitive force sensing experiments where the transduction has to be as efficient as possible. Usually, the mechanical motion is directly converted into a voltage which subsequently undergoes amplification with high gain. A strategy to improve the detection sensitivity is to preamplify the motional amplitude before the electrical conversion using the parametric effect.[10]

Parametric amplification in mechanical resonators has been intensively studied.[10−22] It not only is employed to amplify mechanical signals but also allows for the enhancement of the quality factor,[13,17,22] the storage and the operation of mechanical bits,[16] thermal noise squeezing,[10,20,21] and the reduction of the parasitic signal in capacitive detection schemes.[11] In its most conventional form, parametric amplification consists of modulating the resonator spring constant k_0 at twice the resonant frequency f_0.[23] This is achieved in many NEMS resonators by tuning k_0 electrostatically with a voltage V_g applied on a nearby gate. Nanotube resonators are expected to be excellent candidates for parametric amplification because k_0 can be modulated with V_g by a very large amount: the modulation can be made larger than in any other mechanical resonators fabricated to date (this can be quantified by measuring the V_g dependence of the resonance frequency, which scales as $(k_0)^{1/2}$). However, parametric amplification in a nanotube resonator could not be realized thus far. One

reason for this is that the employed transduction schemes[3,24] are not suitable for such measurements (see below).

Here, we report on a new version of the mixing technique[3] that detects the two quadratures of the motion of a nanotube resonator. This allows us to study the parametric amplification of the motion and to demonstrate a gain as high as 18.2 dB. When k_0 is modulated above a threshold value, the nanotube is shown to enter a regime of instability and self-oscillation; that is, the nanotube oscillates even though the driving force is set to zero.

Our nanoresonators consist of a suspended carbon nanotube clamped between two metal electrodes (Figure 1a) and are fabricated as follows: a trench is etched into a highly resistive Si wafer coated with SiO_2 and Si_3N_4, and W and Pt are evaporated into the trench to create a gate electrode. In a second lithography step, a continuous line is exposed across the trench. After deposition of W/Pt and lift-off, the line results in the source and drain electrodes separated by the trench (these electrodes are electrically isolated from the gate due to the undercut profile of the Si_3N_4/SiO_2 substrate). An island of catalyst is patterned on the drain (or source) electrode using electron-beam lithography, and nanotubes are grown by chemical vapor deposition. This growth is the last step of the fabrication process, and therefore the nanotubes are not contaminated with residues of the resists and chemicals.[25−27]

The nanoresonator is actuated by applying a voltage V_g^{AC} at frequency f to the gate, which causes a driving force $F \propto V_g^{AC}$. The resulting motion is detected by applying a voltage V_{sd}^{AC} at a
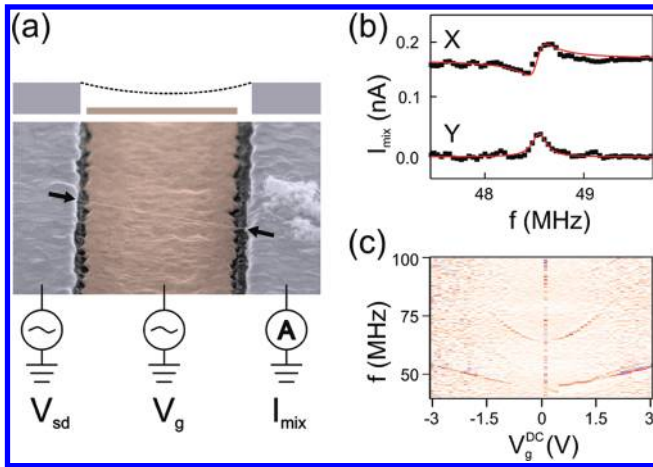
Figure 1. (a) Schematic diagram and false-color scanning electron microscopy (SEM) image of the device. The nanotube (arrows, dashed line in the SEM image) is suspended over a gate electrode (red) between two metal electrodes (gray). The distance between the electrodes is 1 μm. All measurements are performed in an ultrahigh vacuum chamber (about 10^{-10} mbar) at 100 K (in order to avoid the interplay between parametric amplification and Coulomb blockade which emerges at lower temperature). (b) In-phase component X and out-of-phase component Y of I_{mix} (without parametric pumping). The motional amplitude at the resonance frequency is proportional to Y. Red lines are fits using the real and imaginary parts of a Lorentzian. $V_g^{AC} = 5$ mV, $V_{sd}^{AC} = 1.4$ mV. We estimate the motion amplitude to be ~2 nm by comparing the on-resonance signal of Y with the off-resonance signal of X in conjunction with eq 2 as in ref 3. In comparison, the amplitude of the thermal motion is $(k_B T/m(2\pi f_0)^2)^{1/2} = 1.4$ nm (k_B is the Boltzmann constant and we take $m = 7 \times 10^{-21}$ kg the mass of the suspended nanotube). (c) Resonance frequency as a function of gate voltage (from measuring I_{mix} versus f and V_g^{DC}). Two mechanical modes can be seen. All results that follow are obtained for $V_g^{DC} = -1.5$ V and $f \sim 50$ MHz.

slightly detuned frequency ($f - \delta f$) to the source electrode, and by measuring the mixing current I_{mix} at frequency δf from the drain electrode using a lock-in amplifier. In previous works,[3,4,6,7] the recorded signal was the modulus of I_{mix}, which reads

$$I_{mix} = \frac{1}{2} V_{sd}^{AC} \frac{\partial G}{\partial V_g} \left(V_g^{AC} \cos(2\pi\delta ft - \varphi_E) + z_0 V_g^{DC} \frac{C_g'}{C_g} \cos(2\pi\delta ft - \varphi_E - \varphi_M) \right) \quad (1)$$

Here, z_0 is the motional amplitude, $\partial G/\partial V_g$ the transconductance, t the time, V_g^{DC} the constant voltage applied to the gate, C_g the gate–nanotube capacitance, and C_g' its derivative with respect to the displacement. The phase φ_M is the phase difference between the displacement and the driving force, and φ_E is the phase difference between the V_{sd}^{AC} and V_g^{AC} signals. In practice, φ_E is difficult to control (it depends on the details of the measurement circuit such as the cable lengths). Because two phases are at work, the measurement of the modulus of I_{mix} is not convenient to extract z_0. Moreover, we find that φ_E can change with the power of the applied oscillating voltages, which is not suitable for the study of parametric amplification. Other versions of the mixing technique are not appropriate for such a study either. In the frequency-modulation technique,[24] I_{mix} is proportional to the derivative of z_0 with respect to f. In the amplitude-modulation technique,[28] I_{mix} does not measure z_0 at f_0 (since I_{mix} depends only on $\text{Re}[\tilde{z}(f)]$).

We revisit the mixing technique to measure the two quadratures of the motion, $\text{Re}[\tilde{z}(f)]$ and $\text{Im}[\tilde{z}(f)]$. When actuating the resonator with an oscillating force at frequency f, the displacement can be written as $z = \text{Re}[\tilde{z}(f)] \cos(2\pi ft) + \text{Im}[\tilde{z}(f)] \sin(2\pi ft)$ and I_{mix} can take the form (see Supporting Information)

$$I_{mix} = \frac{1}{2} V_{sd}^{AC} \frac{\partial G}{\partial V_g} \left(V_g^{AC} \cos(2\pi\delta ft - \varphi_E) + V_g^{DC} \frac{C_g'}{C_g} \text{Re}[\tilde{z}(f)] \cos(2\pi\delta ft - \varphi_E) \right.$$
$$\left. + V_g^{DC} \frac{C_g'}{C_g} \text{Im}[\tilde{z}(f)] \sin(2\pi\delta ft - \varphi_E) \right) \quad (2)$$

For a properly tuned phase of the lock-in amplifier, the out-of-phase component of the lock-in amplifier output, Y, corresponds to the imaginary part of the resonance (third term in eq 2) and the in-phase component, X, to the real part of the resonance (second term in eq 2) added to a constant background which has a purely electrical origin (first term in eq 2). In order to find this phase, we choose a driving frequency far from f_0 and tune the phase of the lock-in amplifier until the measured out-of-phase component is zero. Figure 1b shows the two quadratures of I_{mix} when sweeping f. The red line is a fit with eq 2 of the measurements assuming that the resonator is described as a damped harmonic oscillator. At the resonance frequency, Y is directly proportional to the amplitude of motion ($z_0 = \text{Im}[\tilde{z}(f_0)]$ and $\text{Re}[\tilde{z}(f_0)] = 0$), which is very practical to study parametric amplification.

Before discussing parametric amplification, we characterize the V_g^{DC} dependence of k_0. For this, we measure f_0 as a function of V_g^{DC} (since $k_0 \propto f_0^2$). Figure 1c shows two clearly resolved resonant modes. Their resonance frequency can be tuned to a large extent with V_g^{DC}. This behavior has been attributed to the increase of the elastic tension that builds up in the nanotube as it bends toward the gate with increasing V_g^{DC}.[3] For the lower frequency mode, df_0/dV_g is constant to a good accuracy over several volts and equal to 4.9 MHz/V. Compared to other NEMS resonators, this response is exceptionally high. Previous studies attained up to $df_0/dV_g = 2$ kHz/V with capacitive forces,[10,13] 240 kHz/V using the Lorentz force,[19] up to 40 kHz/V for piezoelectric NEMSs,[16,17,21,22] and 10 kHz/V using a dielectric force setup.[18] Recently, $df_0/dV_g = 1.1$ MHz/V was obtained by coupling a resonator to a Cooper pair box at very low temperature (130 mK).[20] The high values of df_0/dV_g achieved in nanotube resonators (up to 10 MHz/V at room temperature in ref 3) makes them excellent candidates for parametric amplification.

In order to realize parametric amplification, we apply an additional oscillating voltage V_P at a frequency $2f$ to the gate. On resonance, this modulates k_0 at $2f_0$, thereby achieving parametric pumping of the resonator. We measure the resulting amplification of z_0 by comparing Y_{pumped} to the unpumped signal $Y_{unpumped}$. Figure 2a shows that the mechanical amplification $\Lambda = Y_{pumped}/Y_{unpumped}$ depends on the phase $\Delta\phi$ of the driving force with respect to the pump excitation. The maximum amplification is achieved at about $\Delta\phi = -45°$. We plot the gain corresponding to the amplification at this phase as a function of V_P in Figure 2b. The largest gain is 18.2 dB and is obtained for $V_P = 11.5$ mV. Beyond this pumping voltage, we find that the signal becomes highly unstable.

We analyze our data in the framework of the parametric excitation of a damped resonator. From ref 23, we find that the
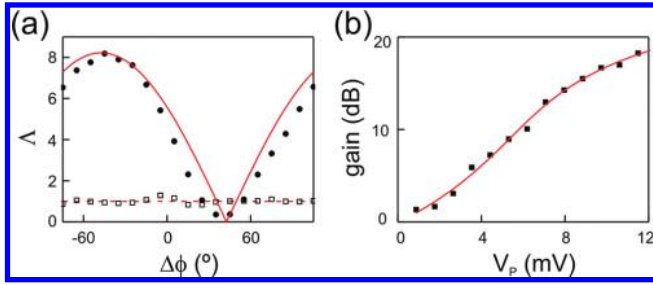
Figure 2. (a) Amplification ($\Lambda = Y_{\text{pumped}}/Y_{\text{unpumped}}$) as a function of the phase difference $\Delta\phi$ between the driving force and the pump for $V_P = 11.5$ mV (solid dots) and $V_P = 0$ (hollow squares). $V_g^{AC} = 3$ mV and $V_{sd}^{AC} = 1.4$ mV. The solid red line is a fit with eq 3. The dashed red line is the mean value when the pump is off. Our measurement setup can only control the shift of $\Delta\phi$; we have determined $\Delta\phi = 0$ from optimizing the agreement between experiment and theory. (b) Gain as a function of the amplitude of V_P for $\Delta\phi$ at which the amplification is largest. The solid red line is a fit with eq 4. $V_g^{AC} = 3$ mV and $V_{sd}^{AC} = 1.4$ mV. We estimate the motion amplitude to be ~10 nm at the largest gain.

amplification is

$$\Lambda = \left| \text{Im}\left[-e^{i\pi/4}\left(\frac{\cos(\Delta\phi + \pi/4)}{1 - V_P/V_{P,C}} + i\frac{\sin(\Delta\phi + \pi/4)}{1 + V_P/V_{P,C}} \right) \right] \right| \tag{3}$$

Here, $V_{P,C}$ is the critical pumping voltage for which the amplification is expected to diverge ($V_{P,C} = (f_0 \ dV_g/df_0)/Q_0$ with Q_0 the quality factor associated to the damping force $\gamma\dot{z}$, where $\dot{z}$ is the velocity). We compare the measurements to eq 3 using $V_{P,C}$ as a fitting parameter (Figure 2a, solid red line). The agreement is reasonable and we obtain $V_{P,C} = 12.5$ mV. (We note that the linear model used for eq 3 is not strictly valid for large V_P, see below.)

Regarding the V_P dependence of the amplification in Figure 2b, the measured amplification tends to saturate at high V_P. This is in opposition to the divergent growth expected from eq 3, which assumes that damping is described by the linear force $\gamma\dot{z}$. According to the theory of parametric amplification,[23] the saturation can be accounted for by adding a nonlinear damping force $\eta z^2\dot{z}$ to the Newton equation of a harmonic oscillator. This force leads to saturation because the associated energy dissipation depends on the amplitude, i.e., higher amplitudes correspond to higher loss of energy. This nonlinear damping force, which naturally emerges from a nonlinear Caldeira−Leggett model,[29] has recently been shown to be crucial to explain the measured driven resonances of nanotube resonators[9] (more discussion on this force can be found below). Following previous work[20,23] the saturation can be quantified by finding the solution Λ of the equation
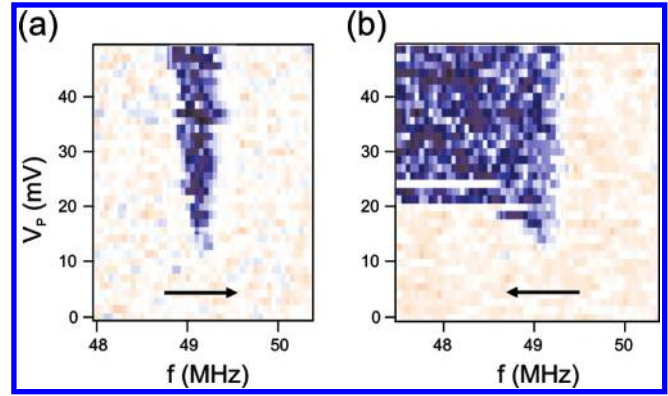
$$V_P = u\Lambda^2 - \frac{v}{\Lambda} + V_{P,C} \tag{4}$$

Here

$$u = \frac{\pi\eta Q_0 f_0 V_{P,C}}{k_0} \text{Im}[\tilde{z}(\omega)]^2_{\text{unpumped}}$$

and

$$v = \frac{Q_0 F V_{P,C}}{\sqrt{2}k_0 \text{Im}[\tilde{z}(\omega)]_{\text{unpumped}}}$$

Figure 3. Parametric self-oscillation (blue) when the pumping frequency is swept upward (a) and downward (b) (by measuring I_{mix} as a function of the detection frequency f and V_P). The driving force at frequency f is set to zero. The observed hysteresis is due to a (negative) Duffing force. In these frequency sweeps, the phase difference between V_P and V_{sd}^{AC} is not kept fixed so the measured I_{mix} is fluctuating. $V_{sd}^{AC} = 1.4$ mV.

where F denotes the driving force. The measurements are compared to the solution of eq 4 using u, v, and $V_{P,C}$ as fitting parameters (solid red line in Figure 2b). The agreement is good and we obtain $V_{P,C} = 7.5$ mV, which is rather similar to the value found above.

With increase in the pump excitation, the nanotube is observed to self-oscillate (Figure 3). That is, the nanotube resonator enters in a regime where it vibrates without any driving force: an immobile resonator is expected to be instable when parametrically pumped with a voltage above $V_{P,C}$, and any fluctuation will activate the oscillating motion.[23] In the measurements, we set $F = 0$ (by putting the oscillating voltage V_g^{AC} at frequency f to zero) and we measure the mixing current as a function of V_P and pump frequency. Figure 3a shows mechanical motion in a tongue-shaped region, which is a typical signature of self-oscillation.[11,15,16,20,22,23] When the pump frequency sweeps in the opposite direction, the measurement is different (Figure 3b); the hysteresis is attributed to a (negative) Duffing force.[16] In both sweep directions, self-oscillation is observed for V_P roughly above $V_{P,C} = 10$ mV. On a technical note, the motion is detected because we apply the voltage V_{sd}^{AC} at frequency $(f - \delta f)$ with $\delta f = 10$ kHz. Although δf is lower than the resonance width (about 150 kHz at low drive, see below), it is unlikely that the voltage V_{sd}^{AC} with frequency $f - \delta f$ affects the measurements in Figure 3 for the following reasons: first, V_{sd}^{AC} is low (1.4 mV) and the corresponding force is not enough to actuate the resonator in a detectable way (the resonance is detected when the drive is equal to or larger than 3 mV). Second, the nanotube resonator behaves as expected in the self-oscillation regime. Namely, we observe no mixing current when the pumping voltage is below the threshold value $V_{P,C}$ and, in addition, the region in which we detect motion has the tongue-shape characteristic of parametric self-oscillation.

In these measurements of parametric amplification and self-oscillation, we obtain three individual estimations of $V_{P,C}$ that are rather similar (about 10 mV). Using $Q_0 = (f_0 \ \partial V_g/\partial f_0)/V_{P,C}$ this corresponds to a quality factor of about 1000. Surprisingly, this is significantly larger than the quality factor obtained when the pump is off (e.g., in Figure 1b where the quality factor is extracted by comparing the resonance line shape with the predictions of a
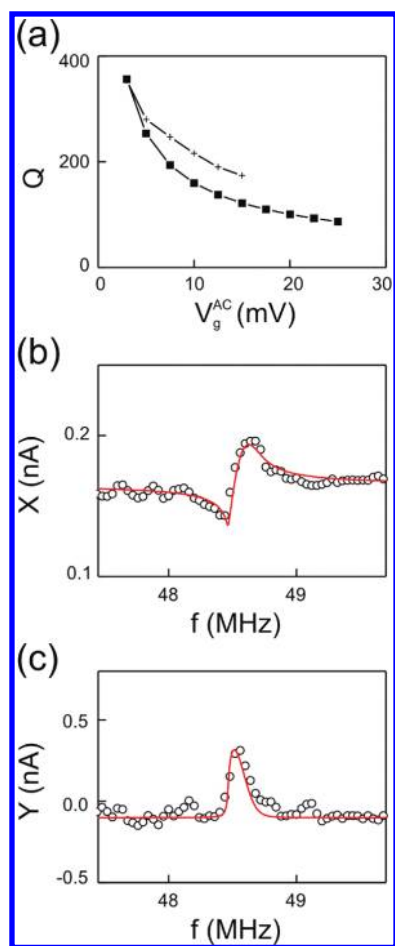
Figure 4. (a) Quality factor as a function of the driving voltage V_g^{AC} in the absence of parametric pumping. The crosses correspond to the quality factor obtained by fitting the resonance line shape with the predictions of a damped harmonic oscillator. The filled squares are obtained by fitting the resonance lineshapes of Y with the solution of eq 5 with a single value for α and η for the different driving forces ($\eta = 120 \, \text{kg} \cdot \text{m}^{-2} \cdot \text{s}^{-1}$, $\alpha = -1.4 \times 10^{10} \, \text{kg} \cdot \text{m}^{-2} \cdot \text{s}^{-2}$, $\gamma = 0$). (b, c) Comparison of the resonance lineshapes of the in-phase component X and the out-of-phase component Y of I_{mix} with the solution of eq 5. $V_g^{AC} = 5$ mV and $V_{sd}^{AC} = 1.4$ mV.

damped harmonic oscillator). There, the quality factor is about 170−350 (crosses in Figure 4a). Measurements on a second resonator give the same results (see Supporting Information). We attribute this difference to the different damping forces that are at work: $\gamma \dot{z}$ and $\eta z^2 \dot{z}$. The experiments on parametric amplification and self-oscillation are sensitive to the critical pump excitation $V_{P,C}$, which is a direct measure of γ. However, $V_{P,C}$ does not necessarily quantify the total damping in the resonator. Indeed, we recently showed[9] that the principal contribution to the damping in a nanotube resonator can stem from the $\eta z^2 \dot{z}$ force. In this case, the quality factor Q estimated from the resonance line shape is lower than $Q_0 = k_0/2\pi f_0 \gamma$ obtained from $V_{P,C}$, which is in agreement with our findings. In the following, we give further experimental evidence that the damping in the studied resonator indeed emanates from the $\eta z^2 \dot{z}$ force. Panels b and c of Figure 4 show that the measured resonance line shape compares reasonably well with the predictions of a Duffing resonator with nonlinear damping, the

equation of motion being described by[9]

$$m\ddot{z} = -k_0 z - \gamma \dot{z} - \alpha z^3 - \eta z^2 \dot{z} + F \cos(2\pi f t) \quad (5)$$

The whole set of resonance lineshapes measured at different driving forces can be fitted with a single value for α and η. The corresponding value of Q depends on the driving force (squares in Figure 4a), which signals that the damping is nonlinear, as demonstrated in ref 9.

An important step forward would be to optimize nanotube resonators in order to further enhance the parametric gain. Since the theory of parametric amplification predicts that the gain is limited by nonlinear damping,[23] methods to reduce this nonlinear damping force should be developed. This is of primary importance since the same nonlinear damping also sets the quality factor of driven nanotube resonators.[9] The microscopic origin of the nonlinear damping is not clear, but it could be related to phonon tunneling, sliding at the contacts, nonlinearities in phonon−phonon interactions, or contamination in combination with geometrical nonlinearities.[9] We will experimentally study the dependence of the nonlinear damping force on contamination, the clamping configuration, and the suspended length. Theoretical work on the microscopic nature of nonlinear damping will prove useful.[29,30]

In conclusion, we demonstrate parametric amplification and self-oscillation in a carbon nanotube resonator. Our results hold promise for ultralow force sensing experiments. We recently demonstrated a force sensitivity of 2.5 aN·Hz$^{-1/2}$ with a nanotube resonator (without parametric amplification)[9] and if it were possible to achieve with this resonator the same gain as reported in the present work, this would surpass the record force sensitivity of 0.51 aN·Hz$^{-1/2}$ recently demonstrated in ref 31. Moreover, nanotube mechanical resonators are promising systems for future studies of the interplay between parametric amplification and Coulomb blockade.[32]

■ ASSOCIATED CONTENT

⑤ Supporting Information. Derivations of eqs 2, 3, and 4 and measurements of self-oscillation from a second resonator. This material is available free of charge via the Internet at http://pubs.acs.org.

■ AUTHOR INFORMATION

Corresponding Author
*E-mail: adrian.bachtold@cin2.es.

■ ACKNOWLEDGMENT

■ REFERENCES

(1) Garcia-Sanchez, D.; San Paulo, A.; Esplandiu, M. J.; Perez-Murano, F.; Forro, L.; Aguasca, A.; Bachtold, A. *Phys. Rev. Lett.* **2007**, *99*, 085501.

(2) Purcell, S.; Vincent, P.; Journet, C.; Binh, V. *Phys. Rev. Lett.* **2002**, *89*, 276103.

(3) Sazanova, V.; Yaish, Y.; Üstünel, H.; Roundy, D.; Arias, T. A.; McEuen, P. L. *Nature* **2004**, *431*, 284.

(4) Lassagne, B.; Tarakanov, Y.; Kinaret, J.; Garcia-Sanchez, D.; Bachtold, A. *Science* **2009**, *325*, 1107.

(5) Steele, G. A.; Hüttel, A. K.; Witkamp, B.; Poot, M.; Meerwaldt, H. B.; Kouwenhoven, L. P.; van der Zant, H. S. J. *Science* **2010**, *325*, 1103.

(6) Lassagne, B.; Garcia-Sanchez, D.; Aguasca, A.; Bachtold, A. *Nano Lett.* **2008**, *8*, 3735.

(7) Chiu, H.-Y.; Hung, P.; Postma, H. W. Ch.; Bockrath, M. *Nano Lett.* **2008**, *8*, 4342.

(8) Jensen, K.; Kim, K.; Zettl, A. *Nat. Nanotechnol.* **2008**, *3*, 533.

(9) Eichler, A.; Moser, J.; Chaste, J.; Zdrojek, M.; Wilson-Rae, I.; Bachtold, A. *Nat. Nanotechnol.* **2011**, DOI: 10.1038/NNANO.2011.71 (published online May 15).

(10) Rugar, D.; Grütter, P. *Phys. Rev. Lett.* **1991**, *67*, 699.

(11) Turner, K. L.; Miller, S. A.; Hartwell, P. G.; MacDonald, N. C.; Strogatz, S. H.; Adams, S. G. *Nature* **1998**, *396*, 149.

(12) Dâna, A.; Ho, F.; Yamamoto, Y. *Appl. Phys. Lett.* **1998**, *72*, 1152.

(13) Carr, D. W.; Evoy, S.; Sekaric, L.; Craighead, H. G.; Parpia, J. M. *Appl. Phys. Lett.* **2000**, *77*, 1545.

(14) Yu, M.-F.; Wagner, G. J.; Ruoff, R. S.; Dyer, M. J. *Phys. Rev. B* **2002**, *66*, 073406.

(15) Shim, S.-B.; Imboden, M.; Mohanty, P. *Science* **2007**, *316*, 95.

(16) Mahboob, I.; Yamaguchi, H. *Nat. Nanotechnol.* **2008**, *3*, 275.

(17) Mahboob, I.; Yamaguchi, H. *Appl. Phys. Lett.* **2008**, *92*, 173109.

(18) Unterreithmeier, Q.; Weig, E. M.; Kotthaus, J. P. *Nature* **2009**, *458*, 1001.

(19) Karabalin, R. B.; Feng, X. L.; Roukes, M. L. *Nano Lett.* **2009**, *9*, 3116.

(20) Suh, J.; LaHaye, M. D.; Echternach, P. M.; Schwab, K. C.; Roukes, M. L. *Nano Lett.* **2010**, *10*, 3990.

(21) Mahboob, I.; Flurin, E.; Nishiguchi, K.; Fujiwara, A.; Yamaguchi, H. *Appl. Phys. Lett.* **2010**, *97*, 253105.

(22) Karabalin, R. B.; Masmanidis, S. C.; Roukes, M. L. *Appl. Phys. Lett.* **2010**, *97*, 183101.

(23) Lifshitz, R.; Cross, M. C. *Reviews of Nonlinear Dynamics and Complexity*; Wiley-VCH: New York, 2008; Vol. 1 [www.tau.ac.il/~ronlif/pubs/RNDC1-1-2008-preprint.pdf]

(24) Gouttenoire, V.; Barois, T.; Perisanu, S.; Leclercq, J.-L.; Purcell, S. T.; Vincent, P.; Ayari, A. *Small* **2010**, *6*, 1060.

(25) Cao, J.; Wang, Q.; Dai, H *Nat. Mater.* **2005**, *4*, 745.

(26) Hüttel, A. K.; Steele, G. A.; Witkamp, B.; Poot, M.; Kouwenhoven, L. P.; van der Zant, H. S. J. *Nano Lett.* **2009**, *9*, 2547.

(27) Steele, G. A.; Götz, G.; Kouwenhoven, L. P. *Nat. Nanotechnol.* **2009**, *4*, 363.

(28) van der Zande, A. M.; Barton, R. A.; Alden, J. S.; Ruiz-Vargas, C. S.; Whitney, W. S.; Pham, P. H. Q.; Park, J.; Parpia, J. M.; Craighead, H. G.; McEuen, P. L. *Nano Lett.* **2010**, *10*, 4869.

(29) Zaitsev, S.; Shtempluck, O.; Buks, E.; Gottlieb, O. *Nonlinear Dyn.* **2011**, DOI 10.1007/s11071-011-0031-5

(30) Dykman, M. I.; Krivoglaz, M. A. *Phys. Status Solidi B* **1975**, *68*, 111.

(31) Teufel, J. D.; Donner, T.; Castellanos-Beltran, M. A.; Harlow, J. W.; Lehnert, K. W. *Nat. Nanotechnol.* **2009**, *4*, 820.

(32) Midtvedt, D.; Tarakanov, Y.; Kinaret, J. *Nano Lett.* 2011, *11*, 1439